

Investigation of the process of mixing reagents in the laser chamber of active medium generators of continuous-wave chemical lasers with promising nozzle arrays

A.V. Avdeev, B.I. Katorgin

Abstract. It is shown that the use of a toothed nozzle array in the active medium generator (AMG) of continuous-wave chemical lasers (CWCLs) allows more efficient mixing of reagents to be achieved in the laser chamber than in an AMG with a slit nozzle array. The results of calculations of parameters of the active medium of a DF CWCL operating in the gain regime for the AMG with traditional and promising nozzle array designs are presented. A kinetic model of processes in the DF CWCL active medium is proposed, which allows obtaining a good agreement with the results of measurements of the small-signal gain.

Keywords: continuous-wave chemical laser, active medium generator, nozzle array, toothed nozzle array.

1. Introduction

In this work, nozzle arrays are considered to be promising if they make it possible to intensify the mixing of oxidising gas flows containing atomic fluorine with secondary fuel flows in the laser chamber by increasing the contact area of adjacent jets of these flows. There are several types of nozzle array configurations that provide such an intensification of mixing processes: HYLTE nozzles [1, 2], tripped nozzles [3–5], and toothed nozzles [6]. The manufacturing technology of almost all of the above-mentioned nozzle arrays is much more complicated than the manufacturing technology of a conventional slit nozzle array, which can be attributed to their main disadvantage. To a lesser extent, this disadvantage affects the case of toothed nozzle arrays. An increase in the contact area of the oxidiser with the secondary fuel is achieved here by introducing protrusions (so-called teeth) into conventional nozzles, which begin immediately behind the critical cross section of the nozzle and extend, gradually increasing in height, to the nozzle cutoff.

The purpose of this work is to show that the use of toothed nozzle arrays in an AMG CWCL allows mixing reagents in a laser chamber more efficiently compared to traditional slit arrays, as well as increasing the gain properties of the active medium.

A.V. Avdeev Moscow Aviation Institute (State Technical University), Volokolamskoe shosse 4, 125871 Moscow, Russia;
e-mail: alex021894@mail.ru;

B.I. Katorgin NPO Energomash, ul. Burdenko 1, 141400 Khimki, Moscow region, Russia

Received 13 December 2019; revision received 10 March 2020
Kvantovaya Elektronika 50 (10) 917–921 (2020)
Translated by M.A. Monastyrsky

2. Statement of the problem

When performing numerical calculations of AMG parameters, the configuration of the toothed nozzle array proposed in [6] was considered. The linear dimensions that define the geometric parameters of the array are shown in Fig. 1, and their values in mm) are given in Table 1.

Table 1. Linear dimensions (in mm) of the toothed nozzle array under consideration.

D	H	L_1	L_2	h_1	h_2	D_1	D_2
5.46	1.25	4.3	2.3	0.13	0.085	2.3	1.5

To assess the effect of the presence of teeth in the nozzles of the oxidiser and secondary fuel on the change in the mixing process of reagents in the DF CWCL laser chamber, the results obtained when calculating the characteristics of the toothed and equivalent slit nozzle arrays were compared. An equivalent slit nozzle array is understood as an array in which the degrees of expansion of the oxidiser and secondary fuel nozzles in comparison with the initial toothed array remain unchanged.

The periodic structure of the toothed nozzle array configurations in question allows us, when constructing a three-dimensional description of the gas flow in the nozzles and the laser chamber, to restrict consideration to one period of the nozzles along the z axis and one half-period of the teeth along the y axis (Fig. 2). The selected flow area was divided by a hexagonal array, while in the flow area of the laser chamber, the array was positioned so that the distances between adjacent nodes in all three dimensions were identical.

The boundary conditions at the inlet to the oxidiser nozzle included data on the pressure, temperature values and oxidising gas composition. These data were determined as a result of thermodynamic calculation of the fuel composition used in [6], the molar flow rates of the components of which are presented in Table 2. The obtained temperature T_0 was 1800 K, with mass fractions $C_F = 0.133$, $C_{HF} = 0.141$, $C_{He} = 0.256$, $C_{CF_4} = 0.309$, and $C_{N_2} = 0.138$. It is worth noting that the obtained mass fraction of atomic fluorine turned out to be close to its optimal value according to the criteria given in [7].

In accordance with work [6], the pressure p_0 in the combustion chamber was taken equal to 10 atm; however, the pressure values of 5 and 2 atm in the combustion chamber were also considered.

The temperature T_0 and the pressure at the secondary fuel nozzle inlet were assumed to be 500 K and 3 atm, respectively. The mass fractions of the components, recalculated from their molar flow rates (see Table 2), were as follows:

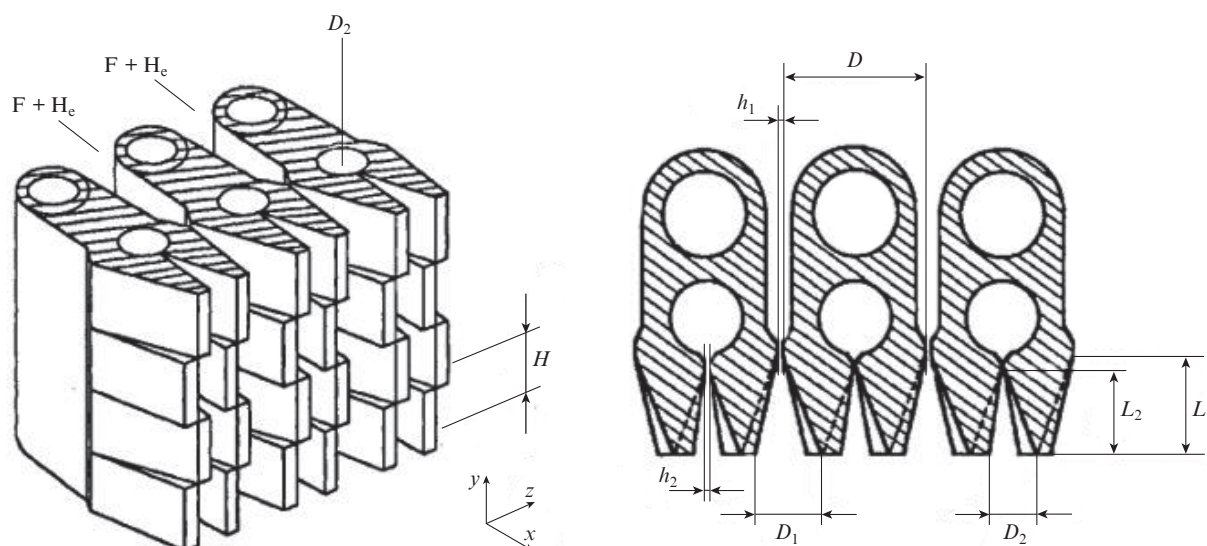


Figure 1. Configuration of a toothed nozzle array.

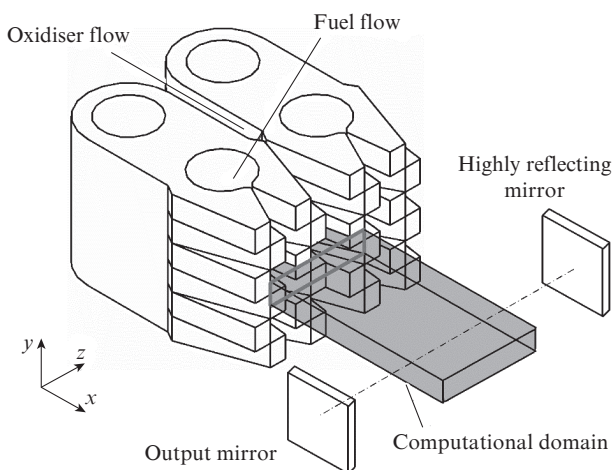


Figure 2. Scheme of the problem statement.

Table 2. Normalised values of molar flow rates of components supplied to the combustion chamber and secondary fuel path (according to work [6]).

Combustion chamber	Secondary fuel path
$G_{\text{NF}_3} = 0.072$	$G_{\text{D}_2} = 0.17$
$G_{\text{C}_2\text{H}_4} = 0.013$	$G_{\text{He}} = 0.249$
$G_{\text{He}} = 0.496$	

$C_{\text{D}_2} = 0.406$, and $C_{\text{He}} = 0.594$. The nozzle wall temperature was also set equal to 500 K.

3. Description of the numerical model. Basic assumptions

The processes occurring in the CWCL active medium, in addition to mixing the jet flows of the oxidiser and secondary fuel, include a multitude of elementary physicochemical transformations that lead to the formation of population inversion at the vibrational–rotational transitions of the HF (DF) molecule. In the presence of an optical resonator, the appearance

of population inversion leads to the generation of radiation and, accordingly, to additional radiation processes occurring in the active medium. For this reason, a rigorous calculation of the energy characteristics and structure of the radiation field in the active medium should be based on the use of a system of gas dynamics equations together with a system of equations for the laser radiation field generated in the optical resonator. In deriving these equations, it is assumed that the CWCL optical resonator is a Fabry–Perot resonator formed by two plane-parallel mirrors. It is assumed that the distribution of HF (DF) molecules over the rotational levels is Boltzmann. In this case (for fast rotational relaxation of molecules), radiation generation in the vibrational bands $v \rightarrow v-1$ in each cross section fixed along the flow only occurs at a single vibrational–rotational transition of the P-branch $v, j_v \rightarrow v-1, j_{v-1}$. In this case, the rotational quantum number j in this cross section is determined by the condition of the maximum gain averaged along the optical axis in the corresponding vibrational band.

The gain is the main characteristic of the active medium, which allows one to evaluate the CWCL energy characteristics. Local value of the gain at a given vibrational–rotational transition of the P-branch $v, j_v \rightarrow v-1, j_{v-1}$ for an HF or DF molecule, defined by the x, y, z coordinates, is calculated as follows:

$$g_{v, v-1}^{j_v, j_{v-1}}(x, y, z, v) = \frac{\rho N_A c^2}{8\pi W_i^2(v_{v, v-1}^{j_v, j_{v-1}})} A_{v, v-1}^{j_v, j_{v-1}} \frac{\theta_{\text{rot}}}{T} \times (2j_{v-1} - 1) f(v_0) \exp\left[-\frac{\theta_{\text{rot}}}{T} j_{v-1}(j_{v-1} - 1)\right] \times \left[C_i(v) - \exp\left(-\frac{2\theta_{\text{rot}}}{T} j_{v-1}\right) C_i(v-1)\right], \quad (1)$$

where ρ is the mixture density; N_A is Avogadro number; c is the speed of light; $A_{v, v-1}^{j_v, j_{v-1}}$ is the Einstein coefficient for spontaneous emission at a given vibrational–rotational transition; W_i is the molecular weight of the i th component; θ_{rot} is the characteristic rotational temperature ($\theta_{\text{rot}}^{\text{HF}} \approx 30$ K, $\theta_{\text{rot}}^{\text{DF}} \approx 15.8$ K); T is the temperature; C_i is the mass fraction of the i th

component; $f(v_0)$ is the function determining the shape of the spectral line with allowance for both Doppler and Lorentzian broadening (at high pressures in the active medium, the contribution of Lorentzian broadening can be significant),

$$f(v_0) = \sqrt{\frac{\ln 2}{\pi}} \frac{2}{\Delta v_D} \exp(a^2) [1 - \operatorname{erf}(a)],$$

$$\operatorname{erf}(a) = \frac{2}{\sqrt{\pi}} \int_0^a \exp(-t^2) dt \text{ is the error function;}$$

v_0 is the centre frequency (in cm^{-1}) of the transition line; $a = \Delta v_L / \Delta v_D \sqrt{\ln 2}$; $\Delta v_D = (2v_0/c) \sqrt{(2RT/W_i) \ln 2}$ (Doppler line width); $\Delta v_L = 5 \times 10^6 p 300/T$ (Lorentz line width); R is the universal gas constant; and p is the pressure in Torr.

The transition probability $v, j_v \rightarrow v-1, j_{v-1}$ is described by the square of the matrix element $R_{v, v-1}$. The Einstein coefficient included in the expression for the gain is related to the matrix element by the expression

$$A_{v, v-1}^{j_v, j_{v-1}} = \frac{64\pi^4}{3h} (v^{j_v, j_{v-1}})^3 \frac{j_{v-1}}{2j_{v-1} - 1} |R_{v, v-1}|^2. \quad (2)$$

Matrix elements for various transitions of the P-branch of HF and DF molecules were most accurately calculated in [8], where the following dependence was proposed:

$$R_{v, v-1} = a_0 + a_1(-j_{v-1}) + a_2(-j_{v-1})^2 + a_3(-j_{v-1})^3. \quad (3)$$

The coefficients a_0, a_1, a_2 and a_3 for calculating the matrix element values are given in Table 3.

To determine the small-signal gain for the toothed nozzle array configuration in question and compare the results obtained with the experimental data presented in [9], we used the relation

$$G_{v, v-1}^{j_v, j_{v-1}}(x) = \frac{1}{h_y h_z} \int_0^{h_y} \int_0^{h_z} g_{v, v-1}^{j_v, j_{v-1}}(x, y, z, v) dy dz, \quad (4)$$

where h_y, h_z are the dimensions of one half-period of the teeth and one period of the nozzles, respectively; and $g_{v, v-1}^{j_v, j_{v-1}}(x, y, z, v)$ is local value of the small-signal gain for a given vibrational-rotational transition of the DF molecule.

4. Results of calculating the mixing of reagents for an AMG in a DF CWCL with different designs of nozzle arrays

The example of the mass fraction distribution of atomic fluorine in Fig. 3a shows a change in the mixing surface at a dis-

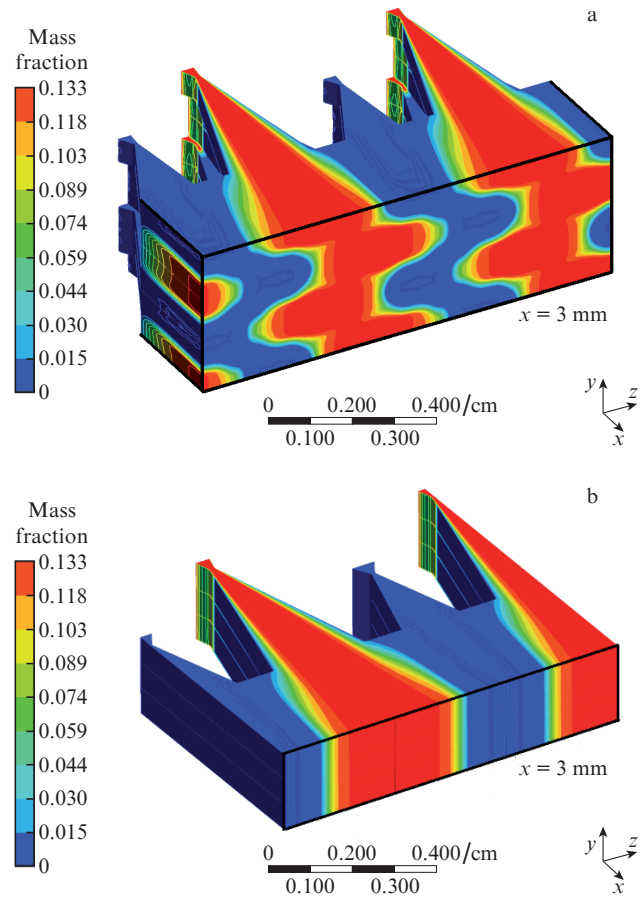


Figure 3. (Colour online) Distribution of the mass fraction of atomic fluorine at a distance of 3 mm from the cutoff of (a) toothed and (b) slit nozzle arrays.

tance of 3 mm from the cutoff of the nozzle array under consideration. For comparison, a similar picture corresponding to the case of an equivalent slit nozzle array is shown in Fig. 3b.

By plotting the concentration distribution of atomic fluorine in the central section of the oxidiser nozzle, we can qualitatively estimate the intensity of the mixing of the components in the laser chamber along the flow. The distribution data obtained for the three considered cases of the pressure in the combustion chamber are shown in Fig. 4. It is seen that with increasing pressure in the combustion chamber and, accordingly, with increasing pressure in the active medium, the mix-

Table 3. Coefficients a_0, a_1, a_2 , and a_3 for calculating matrix elements.

v	HF			
	a_0	a_1	a_2	a_3
1	1×10^{-19}	-2.681×10^{-21}	6.899×10^{-24}	-2.181×10^{-25}
2	1.401×10^{-19}	-3.876×10^{-21}	6.250×10^{-24}	-2.809×10^{-25}
3	1.688×10^{-19}	-4.848×10^{-21}	3.393×10^{-24}	-3.263×10^{-25}
4	1.902×10^{-19}	-5.7×10^{-21}	-5.726×10^{-24}	-3.822×10^{-25}
v	DF			
	a_0	a_1	a_2	a_3
1	8.524×10^{-20}	-1.644×10^{-21}	3.73×10^{-24}	7.126×10^{-26}
2	1.2×10^{-19}	-2.365×10^{-21}	4.191×10^{-24}	8.931×10^{-26}
3	1.456×10^{-19}	-2.942×10^{-21}	3.973×10^{-24}	1.07×10^{-25}
4	1.66×10^{-19}	-3.442×10^{-21}	3.108×10^{-24}	-1.232×10^{-25}

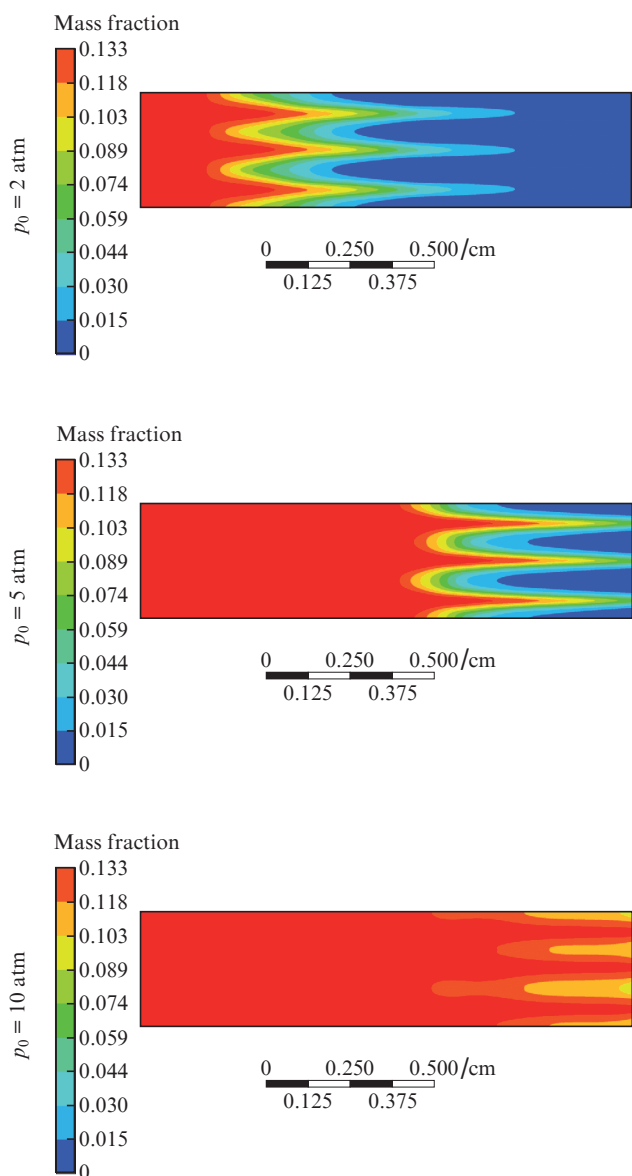


Figure 4. (Colour online) Distribution of the mass fraction of atomic fluorine along the flow of the DF CWCL active medium with a toothed nozzle array in the central plane of the oxidiser nozzle at different pressures in the combustion chamber (zero point is the nozzle array cutoff).

ing zone's length increases. This is explained by a decrease in the diffusion of individual components, which, in turn, leads to a decrease in the rate of secondary fuel penetration into the oxidiser flow's core. However, despite the negative effect of

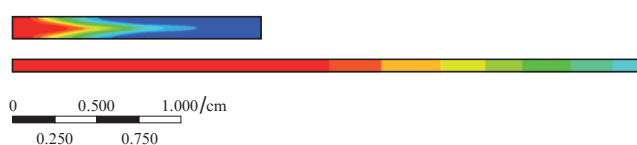


Figure 5. (Colour online) Distribution of the mass fraction of atomic fluorine along the DF CWCL active medium flow with a toothed (with in one half-period along the y axis) and an equivalent slit nozzle array in the central plane of the oxidiser nozzle at a pressure of 2 atm in the combustion chamber.

increasing pressure on the mixing rate, it may be stated that complete mixing of the components in all three cases occurs already at distances of about 2–2.5 cm.

If we consider an equivalent slit array, even at the lowest of the considered pressures in the combustion chamber, the length of the mixing zone of the components will be several times larger (Fig. 5).

Thus, the use of toothed nozzle arrays in the CWCL active medium generator allows more efficient mixing of reagents in the laser chamber compared to the case of slit nozzle arrays.

5. Calculation of the amplifying properties of the DF CWCL active medium with a toothed nozzle array

Using expression (4) and data on the fields of gas-dynamic parameters obtained for the amplification regime using the Ansys CFX software, as well as the toothed nozzle array configuration proposed, the small-signal gain values were calculated at a pressure of 10 atm in the combustion chamber for three vibration–rotational transitions $P_6(2-1)$, $P_8(2-1)$, and $P_7(3-2)$ of the DF molecule in several cross sections along the active medium flow. The choice of these transitions, as in work [9], is explained by the fact that the results of the experi-

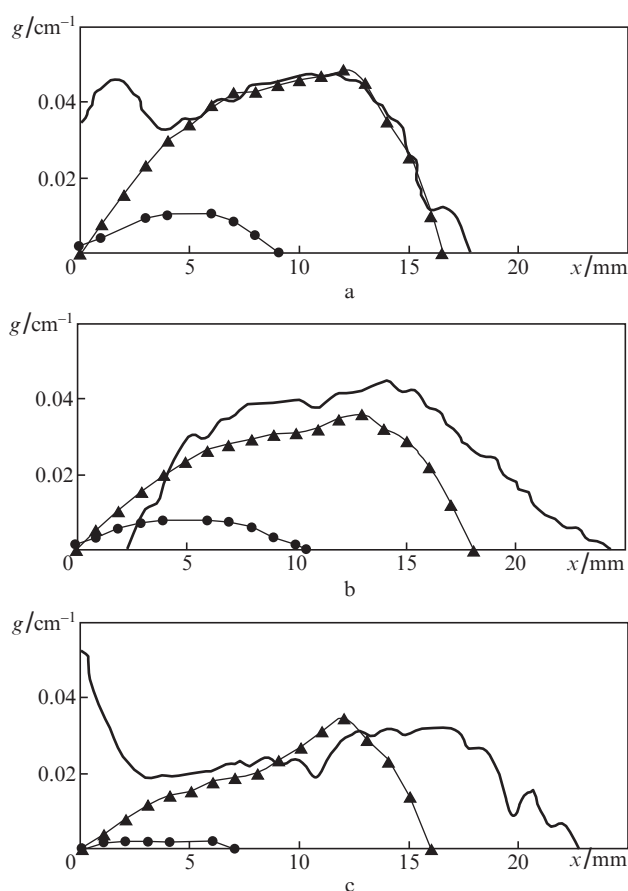


Figure 6. Distributions of the small-signal gain g on the vibrational–rotational transitions (a) $P_6(2-1)$, (b) $P_8(2-1)$, and (c) $P_7(3-2)$ of the DF molecule (solid curves, experiment; \blacktriangle , calculation; and \bullet , calculation with the replacement of the toothed nozzle array by an equivalent slit nozzle array).

mental measurement of the small-signal gain are presented in work [6]. In contrast to [9], the set of rate constants for chemical and relaxation processes (hereinafter referred to as the set of constants) was taken from works [10, 11] rather than from [12]. The obtained distributions of the small-signal gain as a function of the distance from the nozzle array's cross section for three vibrational–rotational transitions of the DF molecule are shown in Fig. 6.

One can see that, in contrast to the data given in work [9], the selected set of rate constants allows us to predict the gain value fairly adequately at all three vibrational–rotational transitions. Significantly lower gain values in the case of a slit nozzle array are due to the small mixing surface area of the adjacent oxidiser and secondary fuel jets and, at the same time, a high pressure in the contact zone (about 20 Torr), at which the diffusion of components is significantly hindered. Such differences in the calculated values of the small-signal gain show how much the introduction of the toothed wall geometry into the slit nozzles of the oxidiser and secondary fuel can improve the gain properties of the active medium under other conditions being the same.

6. Conclusions

1. The proposed kinetic model of the processes in the DF CWCL active medium allowed us to reach a good agreement between the results of using this model and published experimental data on small-signal gain measurements at various vibrational–rotational transitions of the DF molecule, obtained for an AMG with a toothed nozzle array.

2. It is shown that the presence of protrusions in the supersonic part of the oxidiser and secondary fuel nozzles allows more efficient mixing of reagents in the laser chamber in a relatively wide range of pressures compared to the slit nozzle arrays.

3. Significantly lower values of the small-signal gain were obtained when replacing the toothed nozzle array with an equivalent slit nozzle array, which is explained by a lower rate of mixing reagents and, consequently, a lower rate of formation of vibrationally excited DF molecules.

The next step in the study of active medium generators with toothed nozzle arrays may be exploration of the energy characteristics of the CWCL active medium with such arrays.

Acknowledgements. This work has been performed within the framework of the basic part of the State Assignment No. 13.9211.2017/8.9 of the Ministry of Science and Higher Education of the Russian Federation.

1. Hook D., Sollee J. *Techn. Report*, CR-RD-DE-87-15. TRW (1987).
2. <https://www.semanticscholar.org/paper/Review-of-rate-data-for-reactions-of-interest-in-HF-Cohen-Bott/d42fccf3a8a2219b53a3fb6a6ad950f419d7f259>.
3. Wilson L.E. *Proc. SPIE*, **76**, 51 (1976).
4. Driscoll R.J., Tregay G.W. *AIAA Paper*, №81, 1271 (1981).
5. Wilson L.E. *Journal de Physique*, **41**, C9.1 (1980).
6. Voignier F., Merat F., Brunet H. *Proc. SPIE*, **1397**, 297 (1990).
7. Fedorov I.A. *Nepreryvnye khimicheskie lazery na rabochikh molekulakh fluoristogo vodoroda i fluoristogo deyeriya: uchebnoe posobie* (Continuous-wave Chemical Lasers on Working Molecules of Hydrogen Fluoride and Deuterium Fluoride: Textbook) (St. Petersburg: BSTU, 1994) Book 1.
8. Arunan E., Setser D.W., Ogilvie J.F. *J. Chem. Phys.*, **97**, 1734 (1992).
9. Bashkin A.S., Gurov L.V. *Trudy NPO Energomash*, (27), 331 (2010).
10. <https://www.osti.gov/biblio/6445067-review-rate-data-reactions-interest-hf-df-lasers-technical-report>.
11. Gross R., Bott J. *Handbook of Chemical Lasers* (New York, London, Sydney, Toronto: J. Wiley and Sons, 1976; Moscow: Mir, 1980).
12. <https://www.semanticscholar.org/paper/A-Review-of-Rate-Coefficients-in-the-H2-F2-Chemical-Cohen/cbdccf457813f2f50b37a1f097363e65e629eb19>.